SCIENCE CHINA
Physics, Mechanics & Astronomy

• Article •
Special Topic: New Advances in Water and Water Systems

October 2019 Vol. 62 No. 10: 107003
https://doi.org/10.1007/s11433-018-9374-9

Hydrophilic and hydrophobic competition in water-methanol solutions

Domenico Mallamace[1], Sow-Hsin Chen[2], Carmelo Corsaro[1], Enza Fazio[1],
Francesco Mallamace[2,3]*, and H. Eugene Stanley[4]

[1]*Dipartimento MIFT, Università di Messina, Messina I-98166, Italy;*
[2]*Department of Nuclear Science and Engineering, Massachusetts Institute of Technology, Cambridge MA 02139, USA;*
[3]*Istituto dei Sistemi Complessi (ISC) - CNR, Rome 00185, Italy;*
[4]*Center for Polymer Studies and Department of Physics, Boston University, Boston MA 02215, USA*

Received December 11, 2018; accepted February 22, 2019; published online May 31, 2019

We study the thermal behavior of the longitudinal spin-lattice, T_1, and the transverse spin-spin, T_2, relaxation times of the macroscopic magnetization in water/methanol solutions. Our aim is to investigate the reciprocal influence of hydrophobic effects on water properties and of hydrophilicity (via hydrogen bond, HB, interactions) on the solute. Using classical Nuclear Magnetic Resonance spectroscopy, we find a single characteristic correlation time τ_c that reflects all local structural configurations and characterizes the thermal motion effects of the magnetic nuclei on the spin-spin interaction. We find that in the supercooled regime the correlations are stronger, with respect to ambient temperature, because the HB interactions have a lifetime long enough to sustain a stable water network. However, increasing the temperature, progressively decreases the HB interaction lifetime and destroys the water clusters with a consequent decoupling in the dynamic modes of the system. In addition, at temperatures higher than about 265 K, the hydrophobicity becomes gradually stronger and governs the physical properties of the solutions.

hydrophobic-hydrophilic interactions, water systems, thermal properties

PACS number(s): 82.60.Lf, 82.70.Uv, 87.15.Fh

Citation: D. Mallamace, S.-H. Chen, C. Corsaro, E. Fazio, F. Mallamace, and H. E. Stanley, Hydrophilic and hydrophobic competition in water-methanol solutions, Sci. China-Phys. Mech. Astron. **62**, 107003 (2019), https://doi.org/10.1007/s11433-018-9374-9

1 Introduction

Water is essential to life and human activity and is a challenging research subject [1,2]. Compared to other liquids this apparently simple molecule (two atoms of hydrogen and one of oxygen) is thermodynamically anomalous, and there are thus many unanswered questions regarding its dynamic and structural properties [3-7]. It is now clear that intermolecular hydrogen bond (HB) interactions determine the chemical physics of water in both bulk and solution configurations. Each water molecule has two positively charged lobes containing the protons and two lone pairs of electrons. The HB is a non-covalent interaction between an electropositive hydrogen atom on one molecule and an electronegative oxygen atom on a second molecule. The HB is also the result of an important property of water in solutions: molecular hydrophilicity. The HB interaction also governs the local tetrahedral order of water molecules [2]. As water is cooled the HB interaction orders the nearest neighbor molecules, which gradually assume the characteristic four-coordinated geometry. In ordinary ice, each water molecule has four nearest neighbors, a hydrogen donor to two of them and a hydrogen receptor from the other two. In the liquid phase water is also governed by tetrahedrality, but, in contrast to the solid crystalline phase being characterized by a permanent network

---

*Corresponding author (email: francesco.mallamace@unime.it)

© Science China Press and Springer-Verlag GmbH Germany, part of Springer Nature 2019

held together by HB, it is local and transient. Regions of local tetrahedral order can possess a larger specific volume than the overall average. The entropy, on the other hand, always decreases upon cooling because the specific heat is, of necessity, positive. As T decreases, the local specific volume increases due to the progressive increase in tetrahedral order. Water studies of the thermodynamical response functions suggest that when the temperature is decreased the onset of the tetrahedral water patches occurs at $T^* \simeq 320$ K. At higher temperatures the behavior of water is the same as in simple liquids [8].

The opposite property—hydrophobicity—is equally important in science and technology. Hydrophobicity is exhibited when nonpolar substances aggregate in aqueous solution by excluding water. Examples of moieties with these properties characterize amphiphilic molecules (or surfactants). They are usually organic compounds with a head (polar if ionic or HB if non-ionic) in close contact with water molecules and an apolar aliphatic chain, their tails, that avoids water molecules (hydrophobic groups) [9], and although in solutions (water or oil) a single molecule cannot satisfy both of them, a cluster of molecules can, and building blocks of mesoscopic structures can originate under stable thermodynamical conditions [10]. We see a similar situation in many polymers and polyelectrolites that contain both a water-insoluble (or oil-soluble) component and a water-soluble component. This is the "soft condensed matter" research field that focuses on long helical rods (e.g., polypeptides, DNA, RNA, and proteins), discoid organic molecules, polymers, colloids, and many different multimolecular-associated structures (membranes and bilayers) and mesoscopic structures that, despite their complexity, can be described in terms of current statistical physics by means of scaling laws and the concept of universality [11,12].

The hydrophobic effect is as important as the hydrophilic, but its properties have not yet adequately understood. Although several studies addressed the effect solutes have on the structure and energetics of the solvent [13-16], unlike hydrophilicity, which can be fully described in terms of the HB interactions, despite many attempts there are not any analytical forms for quantitatively treating hydrophobicity. For example, a complete experimental measurement of the pair distribution function $g_{AA}(r)$ between hydrophobic molecules (A) lacks, as well as the corresponding potential of mean force $W(r) = -k_B T \ln g_{AA}(r)$ between the two A molecules, i.e., it is necessary to understand the forces underlying hydrophobic interactions, and to evaluate all their implications [17,18]. By means of NMR experiments for the evaluation of the correlation time, we want to give the bases for a theory of hydrophobic effects that is quantitative and that enables the study of complex materials including bio-systems.

In solutions there are solutes with chemical moieties that can change the water HB ordering process, e.g., the ion charge in salt solutions and the hydrophobic heads in simple alcohols and polymer systems. The functions of biosystems, e.g., peptides, proteins, and DNA, are affected by their interaction with water and in particular by the contrast between hydrophilic and hydrophobic metabolites. This means that water is not simply a solvent but is also an integral and active component, i.e., it is itself an important "biomolecule" that plays both a dynamic and structural role [19]. Water interactions—both hydrophilic (HBs) and hydrophobic—are thus key in understanding the properties of water and how water functions not only in biological environments but also in all fields of material science [20].

Molecular Dynamics (MD) simulation studies [21] reveal how hydration forces on the conformation of the shells about a hydrophobic solute can affect the structure of the solute itself. This is scientifically relevant because solute molecules can assume dipole moments that significantly change the solution by changing the thermodynamical variables, i.e., the changes in the solute structure in a solution can strongly effect the hydration thermodynamical functions (entropy and energy) of a hydrophobic solute. Until now these functions have been ascribed to the effect of the solute on the structure of the neighboring water, ignoring the change in the structure of the solute itself. This issue deserves special attention and is one aim of this study.

Using nuclear magnetic resonance (NMR) experiments we find that at the thermal denaturation of an hydrated protein (lysozyme) the hydrophilic (the amide NH) and hydrophobic (methyl CH_3 and methine CH) peptide groups evolve and exhibit different temperature behaviors. This clarifies the role of water and hydrogen bonding in the stabilization of protein configurations [22]. The data also reveal the role of hydrophobic effects in this important protein intramolecular process.

Using these results we study solutions of water and methanol (the smallest amphiphilic molecule) to understand how the mutual hydrophobicity-hydrophilicity affects solution dynamics. We study the solutions at different concentrations and across a wide temperature range from 330 K (near the methanol boiling point) to 200 K. Because the boiling point of methanol is $T_\mathrm{B}^\mathrm{M} = 337.8$ K and the melting point $T_\mathrm{M}^\mathrm{M} = 175.4$ K, at this latter temperature water is in its supercooled regime but methanol is well inside its stable liquid regime. The NMR technique allows a simultaneous study of the separate hydrophilic groups of the two molecules (the hydroxyls of water $\mathrm{OH_W}$ and methanol $\mathrm{OH_M}$ and the methanol methyl groups CH_3 are the only hydrophobic moiety present in solutions). The water methanol solution has been the subject of numerous previous studies that explain the nonlinear behaviors of transport parameters as a function of concentration due to the formation of local structures involving both water and methanol (see, e.g., refs. [23, 24])).

Current models explaining the thermodynamics of liquid bulk water [25, 26], are based on amorphous ice polymorphism [27-29], i.e., on the experimental observation of two glassy phases that differ in density, low density amorphous (LDA) and high density amorphous (HDA), and in their T and P behaviors. The main hypotheses include (1) the stability limit conjecture [30], (2) the singularity-free scenario (SF) [31], and (3) the liquid-liquid phase transition (LLPT) [32]. Both hypotheses (2) and (3) assume that water properties result from the HBs producing a locally-structured transient gel comprised of many molecules that increase in number as the temperature decreases [33, 34]. These local "patches" or HB sub-domains [35,36] enhance the thermodynamical fluctuations (specific volume and entropy and their negative cross-correlations) with anomalies that closely resemble those observed experimentally. The two amorphous states are the corresponding vitreous forms of low-density liquid (LDL) and high-density liquid (HDL). The difference between the SF and the LLPT is that upon supercooling the response functions increase sharply but remain finite in the SF case, but in the LLPT there is a transition with critical fluctuations. The LLPT model also defines a special locus in the P-T plane, the Widom line [37], where the HB network is fully realized, with the LDL phase dominating the HDL. Here the water thermodynamics are characterized by maxima in the response function fluctuations, the corresponding temperature is T_L, and at ambient pressure it is $\simeq$ 225 K [37]. This has been confirmed by experiments in confined water and simulations in bulk water [38-42]. When T is decreased the Widom line converges to the critical point where fluctuations diverge and the LDL phase dominates the liquid structure. We use NMR spectroscopy to study the thermal evolution of the hydrophilic and hydrophobic interactions in these local water HB patches within water-methanol solutions. The goal is to verify whether there are temperature-concentration regions in the solution in which one species dominates the other. Materials and methods are described in Supporting Information.

2 Results and discussion

We study our results using the Bloembergen, Purcell, and Pound (BPP) model (see Supporting Information) that was used to evaluate the thermal behavior of interfacial water confined in hydrophobic nanotubes [43]. We first use the spin-lattice relaxation time, T_1, and the spin-spin relaxation time, T_2, data to obtain the correlation time τ_c. We then study the evolution of the NMR relaxation times as a function of the correlation time τ_c in order to understand the dynamics of the solution molecules and the properties and effects of hydrophilic and hydrophobic interactions. We calculate the correlation time τ_c from the experimental values of the longitudinal and transverse NMR times (T_1 and T_2) according to the BPP model (see eqs. (2) and (3) in Supporting Information) using the quantity T_1/T_2.

Figure 1(a) shows the results as an Arrhenius plot of the correlation times τ_c for pure water (bulk and emulsioned) [44] and methanol (OH and CH_3). Figure 1(b) shows the hydrophilic solution contributions OH_W (water hydroxyl) and OH_M (methanol hydroxyl) and the hydrophobic CH_3 (divided by 10 for figure clarity) for values of the methanol molar fraction in the range $0.1 < X_M < 0.7$ (the symbols are the same as those used in Figure S1).

Note that the solution data differ greatly from those of pure solvent and solute. Note also the behavior of the hydrophilic moieties (of water and methanol) and the hydrophobic solute molecule portion (CH_3). In the hydrophilic moieties there is approximately the same evolution as in the BPP correlation

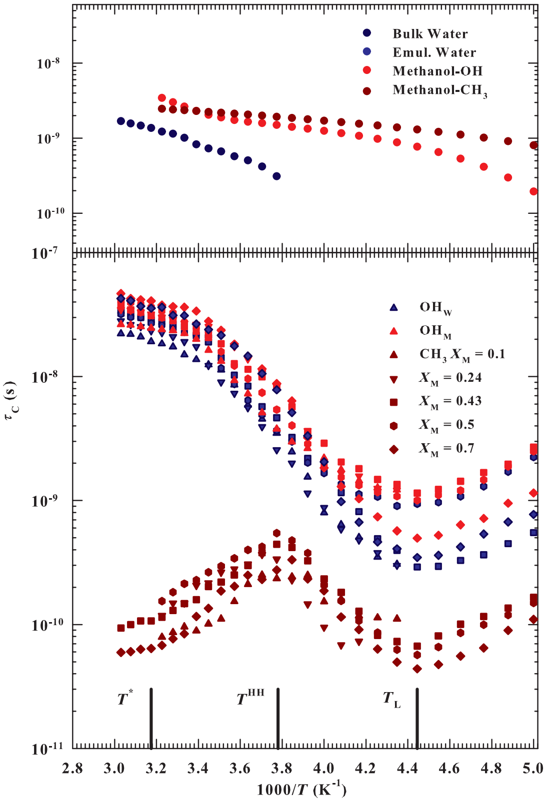

Figure 1 (Color online) Arrhenius plot of the BPP correlation time τ_c calculated from the values of T_1 and T_2, for pure solute and solvent and for some methanol molar fraction in the range $0.1 < X_M < 0.7$ (symbols are the same as those used in Figure S1). (a) The correlation times τ_c corresponding to pure water (bulk and emulsioned) [44] and methanol (OH and CH_3); (b) the hydrophilic solution contributions OH_W and OH_M and the solute hydrophobic part (CH_3, divided by 10 for clarity) are reported.

times corresponding to OH_W and OH_M.

The τ_c data differ for pure water, the solute, and the studied solutions. We see τ_c variations of approximately one order of magnitude when we decrease T in pure water and methanol. Irrespective of their differing T ranges (332-238 K for water and 310-250 K for methanol) the variations are from approximately 2×10^{-9} to 2×10^{-10} s for water, from 3.445×10^{-9} to 1.95×10^{-10} s for the hydroxyl hydrophilic head OH_M of methanol, and 2.46×10^{-9}-8×10^{-10} s for the hydrophobic head CH_3 of methanol. In contrast, the Arrhenius plot of the correlation times of the solution that correspond to the hydrophilic moieties in the range of 332-200 K display three different behaviors when the temperature is decreased. In the first case, there is a moderate decrease from the highest temperature, where $\tau_\text{c}\simeq 4\times10^{-8}$ s up to approximately 315 K ($\tau_\text{c}\simeq 2\times10^{-8}$ s). In the second step, as T decreases there is a decrease in τ_c that is more rapid than in pure water (Figure 1(a)) that starts and evolves in a non-Arrhenius way and ends with a minimum at ~225 K where $\tau_\text{c}\simeq 4\times10^{-10}$ s. In the third step, it slowly increases up to the last measured temperature. Figure 1(b) shows that in the high temperature region the correlation times of both hydroxyl groups are approximately the same, and that at the lowest T the correlation times corresponding to the OH_M are about twice than those of the corresponding OH_W. Note that, in 1964 Hertz and Zeidler [45] found that NMR relaxation times indicated how the reorientation times of the water molecules, that neighbor a solute with alkyl groups, are twice as long as those in pure water, and that the activation energy of the reorientation in the presence of the solute is greater than that in pure water.

The thermal evolution of the methanol hydrophobic BPP correlation time is complex because when the temperature is decreased there is first a maximum and then a minimum. The correlation times related to the solute methyl group for all X_M increase from high temperature values of approximately $\tau_\text{c}\simeq 7\times10^{-10}$ s up to approximately 4×10^{-9} s at a maximum located at ~265 K ($1000/T\simeq3.78$ K^{-1}), after which τ_c decreases toward a minimum of 5×10^{-10} s near ~225 K. Finally it increases to 1.5×10^{-9} s at 200 K. Thus the relaxation time of the solute methyl group varies within an order of magnitude that ranges from 5×10^{-10} to 5×10^{-9} s. We recall here that τ_c data of CH_3 group in solution reported in Figure 1 are divided by 10 for clarity. Note that the maximum temperature in the solution methyl correlation time corresponds to the flex point of the τ_c data for the hydroxyl groups of water and methanol.

Thus the dynamical behavior of the solution exhibits three characteristic temperatures, $T^*\simeq315$ K, $T^\text{HH}\simeq265$ K, and $T_\text{L}\simeq225$ K. The T^* temperature marks the thermodynamical properties of bulk water in the pressure-temperature plane, i.e., it is the locus of the minima in the water isothermal compressibility $K_T(P,T) = -V^{-1}(\partial V/\partial P)_T$ for all the pressures and also the crossing point of the thermal expansion $\alpha_P(P,T) = -V^{-1}(\partial S/\partial P)_T$. Note that $(\partial\alpha_P/\partial P)_T = -(\partial K_T/\partial T)_P$ and that the compressibility represents the volume fluctuations $K_T = \langle\delta V^2\rangle_{P,T}/k_\text{B}TV$. The thermal expansion represents the entropy and volume cross-correlations $\langle\delta S\delta V\rangle$ and $\alpha_P = \langle\delta S\delta V\rangle/k_\text{B}TV$. Thus by considering this transport quantity to be water self-diffusion we see that the T^* temperature marks the onset of tetrahedral water patches [8,46]. On the other hand, T_L is the locus of the so-called fragile-to-strong dynamical crossover observed in confined water [38] and many other supercooled glass-forming materials [47]. It is also the locus of the Stokes-Einstein violation [38,40-42]. Using these τ_c characteristics and comparing the pure materials (Figure 1(a)) with the related solutions data (Figure 1(b)) we find that adding methanol to water even at very low concentration $X_\text{M}=0.1$, i.e., 9 water molecules and 1 methanol molecule, completely changes the local molecular order of water due to the effect of the solute on the water and viceversa. In particular, the methanol molecules strongly affect the water HBs and their ability to form the tetrahedral network, and at the same time the water influences the solute properties. Figure 1(b) shows how the results of these two effects differ sharply.

We use the BPP model to examine τ_c, the required recovery time for the local molecular equilibrium of a system immersed in a static magnetic field following a radio frequency perturbation applied using NMR. Here the thermodynamic conditions of the pre-existing local order is a strong influence [48-51]. We thus examine how hydrophobicity affects the water HB structure shown in an Arrhenius plot of τ_c for the two hydrophilic moieties (OH_W and OH_M) at different concentrations. Note that these hydroxyl groups can interact with each other via HB and give rise to structures of water and methanol (together or separate). In principle this networking increases when T decreases despite the hydrophobicity effects due to the methanol methyl groups. In the past, ring-like structures formed by water and methanol molecules have been proposed [52]. Using X-ray spectroscopy at room temperature reveals that molecules in the pure liquid methanol are arranged in HB chains and rings with six or eight molecules in equal abundance, but that in water methanol solutions the mixing is incomplete at the microscopic level because water molecules bridge the methanol chains to form rings [53]. This cyclic structure hypothesis has received both support and criticism. Neutron diffraction studies indicate that there are water cages around hydrophobic headgroups [54], but we still do not have a convincing description of the details of the incomplete mixing at the molecular level. In addition, our dynamical data indicate that there are hydrophilic-hydrophobic competition effects on the solute and solvent molecules, and that their thermal evolution can provide information on changes in the intermolecular structures. Although the nature of the local order due to hydrophobicity is an open question, we know that the water tetrahedral network due to HBs increases in stability and size. Figure 1 shows how the HB network and the effect of hydrophobicity on it are behind the definition of τ_c and of its behavior related to the hydroxyl groups as a function of temperature. At the highest temperature (335 K) pure water has a τ_c value of $\approx 2\times10^{-9}$ s. Adding methanol in a ratio of one molecule to about 10 of water, causes an increase in τ_c by approximately one order of magnitude (up to $\sim 3\times10^{-8}$ s). At this temperature the water structure is governed by monomers, dimers, and trimers because the HB lifetime is unable to support tetrahedrons (whose onset takes place at T^* [8, 46]). Thus the addition of a small amount of methanol imposes an additional molecular mobility (or disorder) and the time required for the local equilibrium to recover is longer than in the pure solvent. This increase also holds for methanol (see the behavior of the OH_M groups). Because there can be an HB interaction between the OH_W and OH_M moieties, we see that this dramatic change in the system is a hydrophobic effect caused by the solute methyls. When the temperature is decreased the τ_c of the solution hydroxyl groups adopts an Arrhenius behavior up to $\sim T^*$, after which there is a steep decrease with a flex point at T^{HH} followed by a minimum located at approximately T_L, where the correlation time recovers the value $\sim 2.5\times10^{-10}$ s measured in pure water in the very deep supercooled regime (238 K), i.e., near the temperature at which the HB network dominates [39, 41]. This strongly indicates that in the supercooled regime, as in bulk water, the HB interaction of the hydroxyl groups and the consequent pronounced networking exceeds the hydrophobic effects characteristic of the temperatures above the melting point of water. For temperatures $T < T_L$ and for all the studied concentrations, we see a moderate τ_c increase, probably due to relaxations in the HB clusters of water and methanol molecules. This is supported by the differences observed at the very low temperatures between the hydroxyl correlation times, with the one of methanol higher than the one of water. The T^{HH} temperature is thus directly connected to the solute hydrophobicity and its effect on the solvent, and to the effect of hydrophilicity on the hydrophobic solute (the CH_3 metabolite). Figure 1(b) also shows the corresponding BPP correlation time τ_c for the methyl groups. Note that, when T decreases, the correlation time increases from an average value of $\sim 8\times10^{-10}$ s at the highest temperature to $\sim 4\times10^{-9}$ s at T^{HH}, then decreases to a minimum at T_L (5×10^{-10} s), then there is an increase analogous to that observed for the hydroxyl groups. We thus deduce that the high T increase is caused by the effect of water hydrophilicity on the solute hydrophobic heads. This effect is present at all the temperatures, but is affected by the HB interactions that increase with decreasing T. On the other hand, in the high temperature regions where the HBs are weak and have a short lifetime, the methanol CH_3 are unperturbed and the equilibrium recovery after the NMR perturbation is rapid. At the same time the hydrophilicity determines the water HB structure and the onset of the water network, thus when T decreases the HB network becomes increasingly stable and effective, and its influence on the solute hydrophobic metabolites increases and progressively slows the recovery of their equilibrium. At a certain temperature the HB interaction becomes so dominant that it controls the system dynamics. Figure 1(b) shows that when $T < T^{HH}$, the τ_c measured for all the solution metabolites (hydroxyl and methyl groups) evolves in the same way with approximately the same value. In fact, inspecting these data we find that for this latter T regime all the corresponding data inside the experimental error can be superimposed, i.e., the growing tetrahedral structure of water cages all the alcohol molecules at the temperature where the hydrophobic-hydrophilic competition is dominated by the hydrophilic interaction. Thus all these data indicate that in a solution with hydrophilic and hydrophobic molecules a crossover temperature exists and defines two different regions, the high-T region is dominated by hydrophobic interactions and the low-T region is dominated by hydrophilic interactions and by the resulting structures.

Figure 2 shows the BPP plots, i.e., the measured values of T_1 (filled symbols) and T_2 (open symbols) versus the corresponding τ_c in bulk water and methanol. The arrow indicates the increasing temperature. We find that for water (blue data) both the longitudinal T_1 and transverse T_2 relaxation times increase as the correlation time and temperature increase across the studied range. The region around the melting temperature of water T_M is a crossover, below which we find that

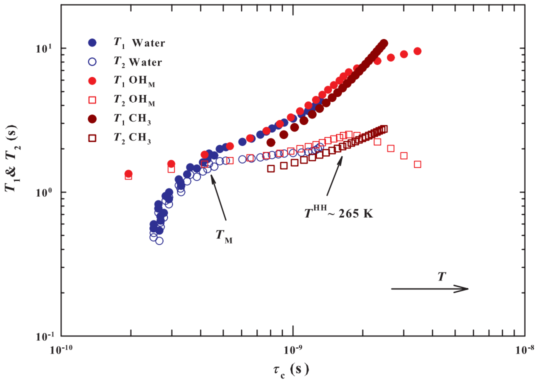

Figure 2 (Color online) The figure illustrates the behaviors of T_1 (full symbols) and T_2 (open symbols) for bulk water (blue) and methanol (red) as a function of the correlation time τ_c. In the solute case these times are reported for the hydroxyl (OH_M) and methyl (CH_3) groups, respectively.

$T_2 \simeq T_1$, and above ($T > T_M$, and τ_c at its higher values) T_1 evolves with a marked increase and T_2 remains nearly constant. The behavior we see below T_M is that predicted by the BPP model. It is the hyperbolic behavior for which $T_2\tau_c$ ~const and $T_2 \simeq T_1$ that is observable under the experimental condition $1/\omega_0 = 1.429 \times 10^{-9}$ s $\gg \tau_c$ (at $\omega_0 = 700$ MHz). This indicates that the HB network becomes increasingly stable as T decreases to well inside the metastable supercooled regime.

We report all the methanol data inside its stable liquid phase and we observe the hyperbolic behavior at the lowest temperature ($T \simeq$205 K). As predicted by the original model, we see that T_1 monotonically increases with increasing τ_c and that the transverse T_2 can either slowly grow or decrease. The data indicate that this occurs only for the hydrophobic group CH_3, and in the high-T regime we see changes in the behavior of the relaxation times corresponding to the hydrophilic OH_M. In particular, at approximately T^{HH} we see a maximum in the spin-spin relaxation time T_2 and also a change in the growth rate of the longitudinal T_1. Note that the transverse relaxation time of the methanol hydroxyl group shows a maximum at the same temperature (middle panel of Figure S1). This confirms that there is also competition between hydrophobic and hydrophilic heads in determining the local order of bulk alcohol. This occurs at a relatively high T for liquid methanol, and the lowered HB lifetime causes the hydrophobicity to dominate the hydrophilic interactions. This is consilient with results obtained for water confined in hydrophobic nanotubes that show how hydrophobicity becomes effective in the high T regime $T > 281$ K [43].

Figure 3 shows the behaviors of T_1 and T_2 as a function of the correlation time τ_c for the solutions at different concentrations of solvent hydroxyls, solute hydroxyls, and solute methyls. Note that the τ_c behaviors of the NMR relaxation times for the OH_W and OH_M hydroxyl groups are similar, e.g., the OH_W data inside the supercooled water regime (Figure 3(a)) are close to the BPP hyperbolic behavior ($T_2\tau_c$ ~const and $T_2 \simeq T_1$) near T_L. In contrast OH_M data (Figure 3(b)) at the same temperature, which now corresponds to the stable methanol liquid phase, are not. For both hydroxyl groups in the high τ_c region, increasing the correlation time changes the longitudinal relaxation time T_1 and produces a crossover between two τ_c behaviors at the corresponding T^{HH}, but in the spin-spin relaxation time this is coincident with the data flex points. We see that T_1 is only slightly dependent on the concentration. Although we cannot fully analyze this, we see that the change in the locus of this T_1 crossover is dependent on the X_M, i.e., on a methanol increase corresponding to an increase in the τ_c of this "crossover". A physical increase in the solute amount causes an additional hydrophobic effect that reduces HB networking, but the error bars disallow verifying this observation.

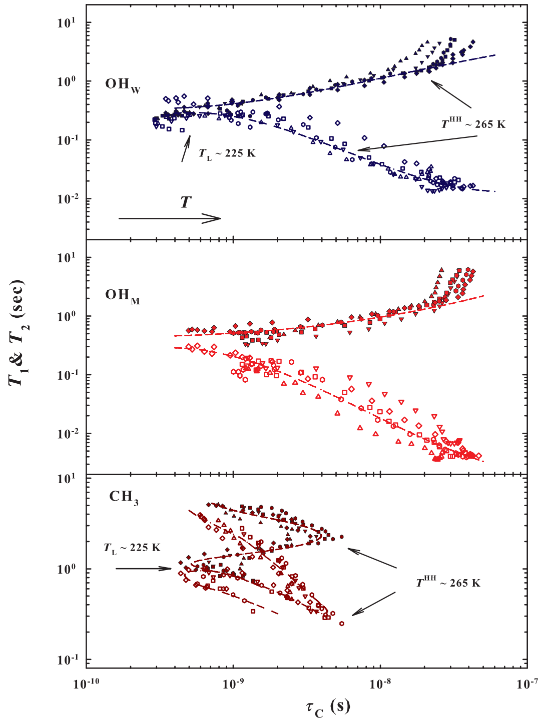

Figure 3 (Color online) The figure illustrates the behaviors of T_1 and T_2 as a function of the correlation time τ_c for OH_W (a), OH_M (b) and CH_3 (c). The symbols are the same as those used previously and all the lines are a guide for eye.

We see that the methanol methyl group relaxation times reported as a function of τ_c (Figure 3(c)) exhibit a cusp-like behavior at both T^{HH} and T_L. This indicates their importance, especially in systems with simultaneous hydrophilic and hydrophobic interactions. The data for the methyl group are mildly dependent on the concentration of the solution, but strongly dependent on the temperature as well as the corresponding transverse NMR relaxation time (bottom panel of Figure S1), and fully reflected in the BPP correlation time. Both are very sensitive to the supercooled water crossover temperature and also to the hydrophobic-hydrophilic interaction thermal balance and thus to T^{HH}. Although low temperature T_L in water indicates the formation of very stable HBs with a tetrahedral network spanning the entire system that causes significant changes in system dynamics, T^{HH} seems to be the temperature above which the hydrophobicity effect dominates in water and water systems. In fact, NMR experiments on water confined inside hydrophobic nanotubes indicate the existence of a hydrophobic-hydrophilic transition around the ambient temperature, demonstrating that the structure of interfacial water on hydrophobic surfaces is temperature-dependent [43]. These observations of water in hydrophobic nanotubes can clarify our results, but additional study is needed to verify the universal character of these behaviors. For example, new studies should clarify how water can influence the biological activity of macromolecules and their folding and unfolding process, and how the onset of ordered structures in water-amphiphilic materials is strongly dependent on system thermodynamics.

3 Conclusions

We have used NMR spectroscopy to investigate the dynamic behavior of water and methanol solutions as a function of temperature—including temperatures in the supercooled regime—and concentration. We have measured the evolution of the longitudinal spin-lattice T_1 and the transverse spin-spin T_2 relaxation times. Within the error bars the data we obtain in bulk solvent and solute agree with literature data. We explore the influence of hydrophobic effects on water properties and the possible influence of solvent hydrophilicity (via HB interactions) on the solute. We use classical approaches to determine how the motion of a given proton in a water molecule is dependent on its nearest neighbors or on the solute. We also examine how solute hydrophobic molecules can be influenced by hydrophilic solvent. In all cases we use the classical approach of a single characteristic correlation time τ_c dependent upon the thermal motion effects of the magnetic nuclei on the spin-spin interaction. We show how the temperature-concentration evolutions of T_1 and T_2 as far as the measured τ_c can be used to explain how the HB interactions that create the characteristic water tetrahedral transient network affect the methanol methyl, and how methanol influences the water structure.

Our study finds two temperature ranges, one dominated by the HB and one typical of the stable liquid states of both water and alcohol in which system properties are driven by hydrophobicity. In the supercooled regime, the τ_c correlation times are strongly correlated because the HB interactions are strong and have a lifetime long enough to sustain a stable water network. Raising the temperature decreases the HB interaction lifetime, destroys the water clusters, decouples the dynamic modes of the system, and hydrophobicity becomes dominant, i.e., when the HB interactions that facilitate clustering in water solutions compete with interactions with opposite behaviors, e.g., hydrophobicity, the effects of these latter interactions become relevant in the temperature regime where the water tetrahedral network is no longer stable.

Thus $\tau_c(T)$ encompasses all local structural configurations, dynamic evolutions, and properties of the solution. We see this reflected in the protons of the different molecular groups of the solvent (OH_W) and solute (OH_M and CH_3). The interaction of the hydroxyls increases the strength and lifetime or stability of the HBs, which in the high T range are influenced by the hydrophobic moieties of the mixture. When we examine the methyl group, the only hydrophobic group within the mixture, we see that, as we decrease T from 335 K, the HB network becomes progressively stronger. When we reach a certain temperature T^{HH}, the mixture dynamics and the corresponding correlations are dominated by the HBs whose networking is fully realized at $T_L \simeq 225$ K for water. These observations reflect the hydrophobic-hydrophilic transition observed in hydrophobic nanotubes as a function of temperature [43]. Note that, unlike such transport functions as viscosity and self-diffusion due to the velocity correlation functions, the NMR correlation time τ_c reflects local correlations on the atomic scale and indicates the existence of a temperature that marks the transition between two different thermal regions: one dominated by the hydrophilicity in which water lies in the metastable supercooled regime, and one located where solute and solvent are both in their stable liquid phase in which the hydrophobicity dominates.In conclusion we have to stress that the used NMR technique essentially looks to the local order of the system so that outstanding challanges for future research are, from one side the exploration of hydrophobic molecules more complex than methanol (polymers or biological macromolecules) and from the other the investigation of the collective effects related to the hydrophobic-hydrophilic interactions. The competition between them is in fact, one of the most challenging research subjects of modern statistical physics. The most important achieved result is the comprehension that these interactions are effective in two different thermal regimes. This circumstance should be seriously considered by MD studies that today essentially constitute the core of these researches.

Francesco Mallamace and all the authors are grateful to Prof. Ben Widom for proposing the important theme of hydrophobicity and for all the suggestions. This work in Massachusetts Institute of Technology was supported by the US Department of Energy (Grant No. DE-FG02-90ER45429). The Boston University work was supported by the National Science Foundation of USA (Grant Nos. CHE-1213217, PHY 1505000, and CMMI 1125290), the Defense Threat Reduction Agency (DTRA) of USA (Grant No. HDTRA1-14-1-0017), and the US Department of Energy (DOE) Contract (Grant No. DE-AC07-05Id14517).

Supporting Information

The supporting information is available online at phys.scichina.com and http://link.springer.com/journal/11433. The supporting materials are published as submitted, without typesetting or editing. The responsibility for scientific accuracy and content remains entirely with the authors.

1 H. E. Stanley, *Liquid Polymorphism* (Wiley, Hoboken, 2013).
2 P. G. Debenedetti, and H. E. Stanley, Phys. Today **56**, 40 (2003).
3 P. G. Debenedetti, *Metastable Liquids* (Princeton University Press,

Princeton, 1997).
4 F. Mallamace, C. Corsaro, D. Mallamace, P. Baglioni, H. E. Stanley, and S. H. Chen, J. Phys. Chem. B **115**, 14280 (2011).
5 F. Mallamace, C. Corsaro, S.-H. Chen, and H. E. Stanley, in *Liquid Polymorphism Volume 152*, edited by H. E. Stanley (John Wiley & Sons, Inc., Hoboken, 2013), p. 203.
6 F. Mallamace, C. Corsaro, D. Mallamace, H. E. Stanley, and S.-H. Chen, in *Liquid Polymorphism Volume 152*, edited by H. E. Stanley (John Wiley & Sons, Inc., Hoboken, 2013), p. 263.
7 P. Kumar, and H. E. Stanley, J. Phys. Chem. B **115**, 14269 (2011).
8 F. Mallamace, C. Corsaro, and H. E. Stanley, Sci. Rep. **2**, 993 (2012).
9 S. A. Safran, *Statistical Thermodynamics of Surfaces, Interfaces and Membranes* (CRC Press, Boca Raton, 1994).
10 P. G. de Gennes, and J. Prost, *The Physics of Liquid Crystals* (Oxford Science Publication, Oxford, 1974).
11 P. G. de Gennes, *Scaling Concepts in Polymer Physics* (Cornell University Press, Ithaca, 1979).
12 P. Flory, *Principles of Polymer Chemistry* (Cornell University Press, Ithaca, 1953).
13 B. Widom, and D. Ben-Amotz, Proc. Natl. Acad. Sci. **103**, 18887 (2006).
14 P. De Gregorio, and B. Widom, J. Phys. Chem. C **111**, 16060 (2007).
15 A. P. Furlan, E. Lomba, and M. C. Barbosa, J. Chem. Phys. **146**, 144503 (2017), arXiv: 1701.08670.
16 D. Corradini, Z. Su, H. E. Stanley, and P. Gallo, J. Chem. Phys. **137**, 184503 (2012).
17 D. Chandler, Nature **437**, 640 (2005).
18 S. Hormoz, and B. Widom, in *Proceedings of the International School of Physics "Enrico Fermi" Course CLXXVI "Complex Materials in Physics and Biology"*, edited by F. Mallamace, and H. E. Stanley (IOS Press, Amsterdam, 2012) p. 1.
19 Y. Levy, and J. N. Onuchic, Annu. Rev. Biophys. Biomol. Struct. **35**, 389 (2006).
20 G. A. Jeffrey, and W. Saenger, *Hydrogen Bonding in Biological Structures* (Springer-Verlag, Berlin, 1991).
21 T. S. van Erp, and E. J. Meijer, J. Chem. Phys. **118**, 8831 (2003).
22 F. Mallamace, C. Corsaro, D. Mallamace, S. Vasi, C. Vasi, P. Baglioni, S. V. Buldyrev, S. H. Chen, and H. E. Stanley, Proc. Natl. Acad. Sci. **113**, 3159 (2016).
23 F. Mallamace, C. Corsaro, D. Mallamace, C. Vasi, S. Vasi, and H. E. Stanley, J. Chem. Phys. **144**, 064506 (2016).
24 N. Micali, S. Trusso, C. Vasi, D. Blaudez, and F. Mallamace, Phys. Rev. E **54**, 1720 (1996).
25 F. Mallamace, Proc. Natl. Acad. Sci. **106**, 15097 (2009).
26 H. E. Stanley, P. Kumar, G. Franzese, L. Xu, Z. Yan, M. G. Mazza, S. V. Buldyrev, S. H. Chen, and F. Mallamace, Eur. Phys. J. Spec. Top. **161**, 1 (2008).
27 O. Mishima, Nature **384**, 546 (1996).
28 O. Mishima, L. D. Calvert, and E. Whalley, Nature **314**, 76 (1985).
29 O. Mishima, L. D. Calvert, and E. Whalley, Nature **310**, 393 (1984).
30 R. J. Speedy, J. Phys. Chem. **86**, 982 (1982).
31 S. Sastry, P. G. Debenedetti, F. Sciortino, and H. E. Stanley, Phys. Rev. E **53**, 6144 (1996).
32 P. H. Poole, F. Sciortino, U. Essmann, and H. E. Stanley, Nature **360**, 324 (1992).
33 H. E. Stanley, J. Phys. A-Math. Gen. **12**, L329 (1979).
34 H. E. Stanley, and J. Teixeira, J. Chem. Phys. **73**, 3404 (1980).
35 A. Geiger, and H. E. Stanley, Phys. Rev. Lett. **49**, 1749 (1982).
36 J. R. Errington, P. G. Debenedetti, and S. Torquato, Phys. Rev. Lett. **89**, 215503 (2002).
37 L. Xu, P. Kumar, S. V. Buldyrev, S. H. Chen, P. H. Poole, F. Sciortino, and H. E. Stanley, Proc. Natl. Acad. Sci. **102**, 16558 (2005).
38 S. H. Chen, F. Mallamace, C. Y. Mou, M. Broccio, C. Corsaro, A. Faraone, and L. Liu, Proc. Natl. Acad. Sci. **103**, 12974 (2006).
39 F. Mallamace, M. Broccio, C. Corsaro, A. Faraone, D. Majolino, V. Venuti, L. Liu, C. Y. Mou, and S. H. Chen, Proc. Natl. Acad. Sci. **104**, 424 (2007).
40 S. Cerveny, F. Mallamace, J. Swenson, M. Vogel, and L. Xu, Chem. Rev. **116**, 7608 (2016).
41 L. Xu, F. Mallamace, Z. Yan, F. W. Starr, S. V. Buldyrev, and H. E. Stanley, Nat. Phys. **5**, 565 (2009).
42 F. Mallamace, C. Corsaro, N. Leone, V. Villari, N. Micali, and S. H. Chen, Sci. Rep. **4**, 3747 (2015).
43 H. J. Wang, X. K. Xi, A. Kleinhammes, and Y. Wu, Science **322**, 80 (2008).
44 F. Mallamace, C. Corsaro, D. Mallamace, S. Vasi, and H. E. Stanley, J. Chem. Phys. **145**, 214503 (2016).
45 H. G. Hertz, and M. D. Zeidler, Ber. Bunsen Ges. Phys. Chem. **68**, 821 (1964).
46 J. H. Simpson, and H. Y. Carr, Phys. Rev. **111**, 1201 (1958).
47 F. Mallamace, C. Branca, C. Corsaro, N. Leone, J. Spooren, S. H. Chen, and H. E. Stanley, Proc. Natl. Acad. Sci. **107**, 22457 (2010).
48 F. Bloch, Phys. Rev. **70**, 460 (1946).
49 E. M. Purcell, H. C. Torrey, and R. V. Pound, Phys. Rev. **69**, 37 (1946).
50 N. Bloembergen, E. M. Purcell, and R. V. Pound, Phys. Rev. **73**, 679 (1948).
51 R. Kubo, and K. Tomita, J. Phys. Soc. Jpn. **9**, 888 (1954).
52 L. Pauling, *The Nature of the Chemical Bond* (Cornell University Press, Ithaca, 1960).
53 J. H. Guo, Y. Luo, A. Augustsson, S. Kashtanov, J. E. Rubensson, D. K. Shuh, H. Ågren, and J. Nordgren, Phys. Rev. Lett. **91**, 157401 (2003).
54 S. Dixit, J. Crain, W. C. K. Poon, J. L. Finney, and A. K. Soper, Nature **416**, 829 (2002).